



Equilibrium Properties of the Mixed State in Superconducting Niobium in a Transverse Magnetic Field: Experiment and Theoretical Model

V. Kozhevnikov¹ · A.-M. Valente-Feliciano² · P. J. Curran³ · G. Richter⁴ · A. Volodin⁵ · A. Suter⁶ · S. J. Bending³ · C. Van Haesendonck⁵

Received: 14 February 2018 / Accepted: 20 February 2018 / Published online: 5 March 2018
© Springer Science+Business Media, LLC, part of Springer Nature 2018

Abstract

Equilibrium magnetic properties of the mixed state in type II superconductors were studied on high-purity film and single-crystal niobium samples with different Ginzburg-Landau parameters in perpendicular and parallel magnetic fields using dc magnetometry and scanning Hall-probe microscopy. The magnetization curve for samples with unity demagnetizing factor (slabs in perpendicular field) was obtained for the first time. It was found that none of the existing theories is consistent with these new data. To address this problem, a theoretical model is developed and comprehensively validated. The new model describes the mixed state in an averaged limit, i.e., without detailing the samples' magnetic structure and therefore ignoring the surface current and interactions between the structural units (vortices). At low values of the Ginzburg-Landau parameter, it converts to the model of Peierls and London for the intermediate state in type I superconductors. The model quantitatively describes the magnetization curve for the perpendicular field and provides new insights into the properties of the mixed state, including properties of individual vortices. In particular, it suggests that description of the vortex matter in superconductors of the transverse geometry as a “gas-like” system of non-interacting vortices is more appropriate than the frequently used solid-like scenarios.

Keywords Superconductors · Mixed state · Magnetization · Thermodynamic properties · Vortices

1 Introduction

Equilibrium bulk magnetic properties of the mixed state (MS) in type II superconductors are discussed in all superconductivity textbooks and in numerous papers which followed after the discovery of type II superconductivity by Shubnikov with coworkers eight decades ago [1].

References for many of these papers can be found, e.g., in [2–5]. However, some fundamental magnetic properties of the MS are still not well understood. Examples include, but are not limited to, the magnetization curve $M(H)$, where M is the magnetic moment and H is the external field, and the field strength H_i (also referred to as the magnetic and magnetizing force [7], the thermodynamic field [8], the Maxwell field [9], etc.) in samples of other than cylindrical geometry. Following Abrikosov [9], under “cylindrical geometry,” we imply infinite right cylinders with base of arbitrary shape (e.g., circular cylinders and slabs) in parallel field, that is samples with demagnetizing factor $\eta = 0$ [6]. Cross-sectional diagram of the cylindrical geometry is shown in Fig. 1a.

Our original interest to equilibrium properties of type II superconductors (that is to properties of pinning-free type II samples) of non-cylindrical geometry and specifically to those with $\eta = 1$ (infinite slabs in transverse, i.e., perpendicular field [6]) was due to the fact that the latter do not have a lateral surface by definition. This automatically excludes effects associated with surface current (including

✉ V. Kozhevnikov
vladimir@itf.fys.kuleuven.be

¹ Tulsa Community College, Tulsa, OK 74119, USA

² Thomas Jefferson National Accelerator Facility, Newport News, VA 23606, USA

³ University of Bath, Bath BA2 7AY, UK

⁴ Max Planck Institute for Intelligent Systems, 70569 Stuttgart, Germany

⁵ Solid State Physics and Magnetism Section, KU Leuven, BE-3001 Leuven, Belgium

⁶ Paul Scherrer Institut, 5232 Villigen PSI, Switzerland

the Meissner state) and surface barriers. Hence, properties of sufficiently thick samples of this kind provide access to the pure bulk properties of the MS, i.e., to properties of the vortex assembly. On the other hand, vortices in such samples are evenly distributed due to symmetry and their number density is strictly calculated from the flux conservation. Thus, properties of these samples may also be used for inferring properties of individual vortices. Therefore, knowledge of equilibrium properties of samples of the transverse geometry (this term will be used for samples with $\eta = 1$) is of fundamental importance. The sample field configuration for the transverse geometry is shown in Fig. 1b.

It is worth noting that real samples of the cylindrical and the transverse geometries are samples with $\eta \rightarrow 0$ and $\eta \rightarrow 1$, respectively. Correspondingly, effects due to the lateral surface are most significant for the former and practically irrelevant for the latter.

Here, we report on the results of an experimental study of thermodynamically equilibrium (i.e., uniquely determined by parameters of state and hence reversible) bulk magnetic properties of the MS, measured on Nb high-purity film and single-crystal samples [10]. Measurements were performed at the field directed both parallel and perpendicular to the samples' plane. To the best of our knowledge, such data for the perpendicular field were not reported before. It turned out that none of the existing theories is consistent with these new data. A theoretical model quantitatively accounting for these data is developed and introduced here as well. Similar to the model of Peierls [11] and London [12, 13] for the intermediate state (IS) of type I superconductors, our model describes the MS in thick samples of any ellipsoidal shape

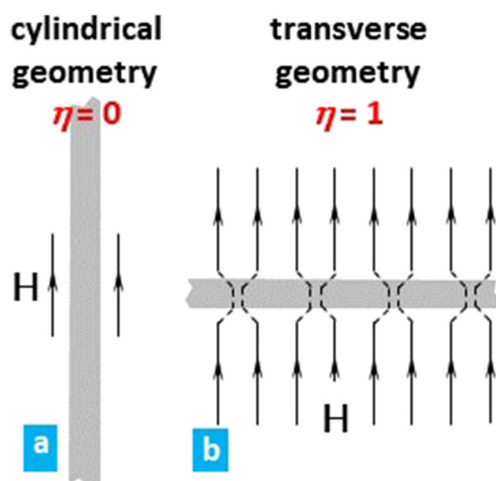


Fig. 1 Schematic diagrams showing cross section of samples (painted in gray) for cylindrical (a) and transverse (b) geometries. η is the demagnetizing factor and H is the external field. Dashed lines (not shown in a) depict the lines of the magnetic induction B near and inside the sample

($0 \leq \eta \leq 1$) in an averaged limit, i.e., without detailing the samples' magnetic structure and therefore ignoring the surface current and interactions between vortices; in other words, following the terminology of de Gennes [8], it accounts for the properties of the MS in zero-order approximation. At low values of the Ginzburg-Landau (GL) parameter κ , our model converts to the model of Peierls and London. We will show that the description of the vortex matter in terms of a system of non-interacting vortices is the most appropriate for samples of the transverse geometry.

2 Problem Status and Motivation

There are two equilibrium states in which superconductors contain domains of normal (N) phase imbedded into superconducting (S) phase. Those are the IS in type I and the MS in type II materials. In the IS, due to positive energy of the S-N interface, the N domains are multi-flux-quantum laminae, whereas in the MS, due to negative interface energy, these domains are single-flux-quantum vortices. This quantitative difference in the flux magnitude results in drastic qualitative differences between properties of type I and type II superconductors. In particular, the MS takes place in samples of any shape including the cylindrical one (i.e., for $0 \leq \eta \leq 1$), whereas the IS occurs only if $\eta \neq 0$ [15]. (By “shapes” we imply shapes of ellipsoids, because only ellipsoids allow rigorous theoretical treatment of the magnetic properties [7].)

For this reason, significant attention was paid to measurements of magnetic properties of cylindrical samples of type II superconductors, which, in particular, led to a fairly good knowledge of the $M(H)$ curve for this geometry [1, 3, 16–19].

For cylinders at $H < H_{c1}$, the Meissner condition $B = 0$ allows one to calculate $M(H)$ in three ways: (i) from thermodynamics, (ii) from magnetostatics (see, e.g., [21]), or (iii) from the Maxwell field H_i , which in this case equals to the applied field H due to continuity of the tangential component of this field [14]. Then, M is calculated from H_i defined (in CGS units) as $H_i \equiv B - 4\pi m$, where B is the induction and m is the magnetization, which in superconductors is a *macroscopic* average M/V , where V is the sample volume [20].

However, in the MS ($H_{c1} < H < H_{c2}$), complexity of current distribution leaves only one option to calculate M , i.e., through the field H_i via calculation of the average induction \bar{B} . Then, $4\pi M/V$ is computed as $\bar{B} - H_i$. For cylinders, where $H_i (= H)$ is known, this was done using the GL theory near H_{c1} and H_{c2} [15], and also with use of the London equation in the vicinity of H_{c1} [9, 22]. In these field regions, approximate analytical expressions for

\bar{B} are available for the extreme type II limit $\ln \kappa \gg 1$ [9, 15, 22]. At the same time, it is supposed that the entire $M(H)$ curve for any κ can be calculated via numerical solution of the GL equations [23]. Note, however, that available approximate [15, 24] and high-precision [25] solutions of the GL equations are not quite consistent with this supposition. For instance, theoretical $M(H)$ exhibits an infinite slope at H_{c1} , whereas the slope of a truly reversible $M(H)$ curve is not infinite [17].

The situation becomes much more complicated for non-cylindrical geometry. For the experiments, this is due to a much larger number of pinning centers in the sample area perpendicular to the field. For that reason, available data on $M(H)$ for type II samples of the transverse geometry (see, e.g., [26–28]) are strongly irreversible and therefore inappropriate for judgment on thermodynamic properties.

On the theoretical side, the main complication is due to a demagnetizing field $\mathbf{H}_d \equiv \mathbf{H} - \mathbf{H}_i$. The Maxwell field H_i can be rigorously calculated for uniform (meaning that B is homogeneous throughout the sample) ellipsoids [2, 6, 7]. If H is parallel to the sample axis, relative to which the demagnetizing factor is η , then,

$$(1 - \eta)H_i + \eta B = H. \tag{1}$$

Therefore,

$$H_i \equiv H - H_d = H - \eta(B - H_i) = H - \eta 4\pi M/V. \tag{2}$$

Thus, in uniform samples, $H_d = \eta 4\pi M/V$. In the Meissner state, the sample is (i) uniform and (ii) $B (= 0)$ is known. The former makes it possible to calculate η (see, e.g., [6]) and the latter allows one to use (1) yielding $H_i = H/(1 - \eta)$. Then, $4\pi M/V \equiv B - H_i = -H/(1 - \eta)$ in full consistency with experiments (see, e.g., [2]). However this is not the case for the MS, where B is not uniform and therefore η is not well defined and neither H_d nor H_i is known.

On the first view, the solution of the problem for η was found long ago by Peierls [11] and London [12] for the IS via replacement of B by \bar{B} , which allows one to use η of the uniform sample. However, (2), which follows from (1), still contains two unknowns (H_i and M) and therefore one more independent relationship is needed to find M . Peierls and London resolve this problem *assuming* that H_i equals to the thermodynamic critical field H_c in the entire field range of the IS. However, this is not applicable for the MS.

One might object that there is the well-known approach for the MS [8, 29] in which H_i for $\eta \neq 0$ is calculated from (1) as $H_i = (H - \eta\bar{B})/(1 - \eta)$ [30]. Then, \bar{B} is calculated using $\bar{B}(H)$ obtained for the cylindrical geometry (referred to as the constitutive relation $B_e(H)$ [29]) replacing H by H_i , and then both $B_e(H_i)$ and H_i are used to compute $4\pi M/V = B_e(H_i) - H_i$.

Apart from knowing $B_e(H)$, the *principal condition* for using this approach is ability to calculate H_i from (1). However, since no new relationship between H_i and M or B is added (see also [6]), this way to compute H_i is questionable. Indeed, for $\eta = 1$, where $\bar{B} = H$ [9, 31, 32], (1) yields $H_i = H(1 - \eta)/(1 - \eta) = H$ and therefore $M = 0$ regardless of H , implying that $H_{c2} = \infty$. The reason of such a striking inadequacy of this approach is very simple: a uniform sample with $\eta = 1$ is just a sample in the N state, where M is indeed zero. In other words, in order to use (1) for inhomogeneous samples, H_i should be found independently, like in the Peierls-London model for the IS ($H_i = H_c$) or in the cylindrical geometry for the MS ($H_i = H$) [15].

In [33, 34] $M(H)$ for films with different κ and thickness d in perpendicular field was calculated using the GL theory. Calculated curves strongly depend on κ and d , but contradict the rule of 1/2 [21] (see more about this rule in the Discussion section below) and hence cannot be completely correct.

The approach based on London equation [22] does not work for the transverse geometry either. Specifically, for cylinders the thermodynamic potential $\tilde{F} \equiv F - BH_i/4\pi = F - BH/4\pi$ is minimized at the expense of the second (negative) term, reflecting the work done by the magnet power supply when the flux through the sample changes. Here F is the Helmholtz potential and \tilde{F} is its Legendre transform, also referred to as the Gibbs free energy [13]. In the transverse geometry the flux is fixed, hence the term $BH_i/4\pi$ is absent [6, 8, 9]. This makes the minimization of $\tilde{F} = F$ impossible, since all terms and their derivatives in F are positive [22].

After all, inhomogeneities of the field and of the vortex cores near the surface perpendicular to the field should be taken into account. These inhomogeneities, unimportant when $\eta = 0$, can be important for films in non-parallel fields, making their properties dependent on the film thickness. For instance, in the IS, they can change the critical field of a few-micrometer-thick film in perpendicular field by more than 50% compared to that in parallel field [21, 35]. An attempt to address this issue for the MS was made by Cody and Miller in experiments with Pb films [28]; however, the results obtained are inconclusive due to strong pinning in their films.

To summarize, (a) available experimental information on the equilibrium magnetic properties of the MS in samples of non-cylindrical geometry is incomplete. In particular, the available $M(H)$ data are strongly irreversible and hence inapplicable for consideration of thermodynamic properties. (b) Available theoretical results and approaches are controversial. In particular, none of the existing theories is capable to address $M(H)$ curve for samples with $\eta = 1$.

Progress toward solution of this fundamental problem is the goal of our work, which results are presented below.

3 Experimental

Fabrication of pinning-free samples, being very challenging for type I materials [2, 21], is even more difficult for type II superconductors, since most of them are alloys with inevitably significant pinning [1, 8]. A single-crystal sample can be a solution, but since we also need a film for verification of dependencies of the properties on the sample thickness, such a solution is not complete.

Nb is known as a well-verified intrinsic type II superconductor [17, 36–38], hence, it is a material from which one can hope to fabricate pinning-free films. On this reason, Nb was chosen for our samples. However, Nb is also a getter [17]. Due to that, our first films, deposited via magnetron sputtering and having residual resistivity ratio RRR up to 70, were still insufficiently clean.

The Nb film sample (Nb-F) used in this work is one of two film samples which were used in [39], where their properties at $H \geq H_{c2}$ are discussed. The film was grown on sapphire via electron cyclotron resonance technique (ECR) [40]; its RRR is 640, the size is $4 \times 6 \text{ mm}^2$, and the thickness is $5.7 \mu\text{m}$. This is a record pure Nb film, of the same purity as In films used in IS studies [21, 35]. For comparison, RRR of ultra-pure 2.5-mm thick Nb sheets used for radio-frequency cavities (RFC) in particle accelerators is ≈ 300 [41]. More about ECR-grown Nb films can be found in [42].

Another sample (Nb-SC) was also a sample used in [39]. It is a one-sided polished single-crystal Nb disc $\varnothing 7 \text{ mm} \times 1 \text{ mm}$ supplied by Surface Preparation Laboratory, The Netherlands. The sample was subjected to a standard treatment used for the RFC fabrication: it was annealed at $800 \text{ }^\circ\text{C}$ for 3 h and electrochemically polished after that.

However, there is one more issue with Nb. A driving force to achieve thermodynamic equilibrium in inhomogeneous samples is the S-N surface tension [21], whose magnitude in type II Nb is significantly less than that in type I In. This could require even purer Nb samples, but fortunately, pinning weakens with temperature T . Specifically, $M(H)$ data for both our samples are close to reversible at $T \gtrsim 8 \text{ K}$, which means that the samples are nearly pinning free at these temperatures. For this reason, we mostly discuss the data obtained at high temperatures.

The magnetic moment was measured using Quantum Design dc magnetometer (Magnetic Properties Measurement System). Most measurements were performed at constant temperature in the following order. After demagnetizing the magnetometer at $T > T_c$ (T_c is the critical temperature), the sample was cooled down to the chosen temperature in zero applied (i.e., in Earth) field. Then, M

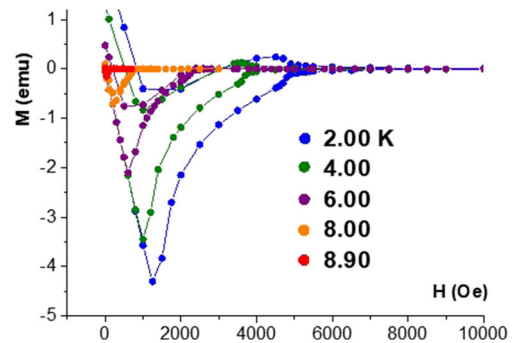


Fig. 2 Data for the magnetic moment of the Nb-SC sample measured in parallel field at temperatures indicated

was measured vs H up to the field well exceeding the critical field H_{c3} , where the last traces of superconductivity were absent. After that, the measurements were continued at descending H down to zero applied field.

Data obtained for the Nb-SC sample in parallel field are shown in Fig. 2 and typical data for high temperatures are presented in Fig. 3. As seen from Fig. 2, in the Meissner state, data for all temperatures agree with each other. Hence, the sample was well aligned with \mathbf{H} and the flux trapped at the ascending field was low, which allows calculating the thermodynamic critical field $H_c(T)$ from the area above $M(H)$ curves [16]. The sample volume calculated from $M(H)$ at $H < H_{c1}$ agrees with that measured directly within 5% error, indicating that $\eta_{\parallel} \lesssim 0.05$ and therefore $\eta_{\perp} = 1 - 2\eta_{\parallel} \gtrsim 0.9$ [6]. Here, η_{\parallel} and η_{\perp} are the demagnetizing factors in parallel and perpendicular fields, respectively.

Data for magnetic moment measured for the Nb-F sample in parallel field are shown in Fig. 4. Typical high-temperature data obtained for this sample are available in [39]. The sample volume was determined from the slope of

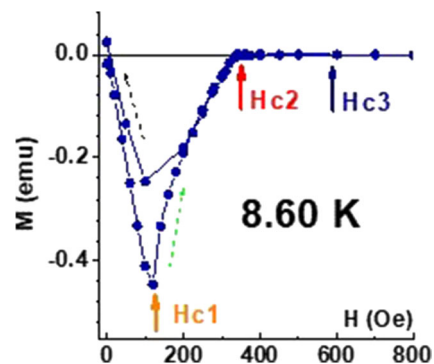


Fig. 3 Data for the magnetic moment of the Nb-SC sample measured in parallel field at $T = 8.60 \text{ K}$. H_{c1} , H_{c2} and H_{c3} designate the respective critical fields. Dashed arrows indicate either the measurements were conducted at ascending (green arrow) or descending (black arrow) field

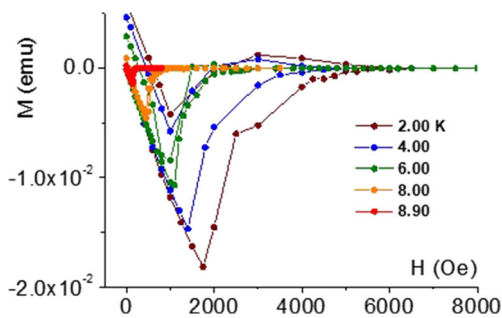


Fig. 4 Data for the magnetic moment of the Nb-F sample measured in parallel field at temperatures indicated

$M(H)$ curves in the Meissner state; its uncertainty is 10%. η_{\perp} of this sample is $1 - O(10^{-3})$ [6].

The $M(H)$ data measured in parallel field were used to construct the phase diagrams necessary for discussion of experimental results for perpendicular field. These phase diagrams are shown in Figs. 5 and 6 for the Nb-SC and the Nb-F samples, respectively. The inserts show the data for M measured vs temperature at Earth field. For the Nb-SC sample, $T_c = 9.20$ K and κ calculated as $H_{c2}/\sqrt{2}H_c$ [15] is 1.3 near T_c increasing to 1.6 at 2 K. For the Nb-F sample, $T_c = 9.25$ K and κ starts from 0.8 near T_c reaching 1.1 at 2 K.

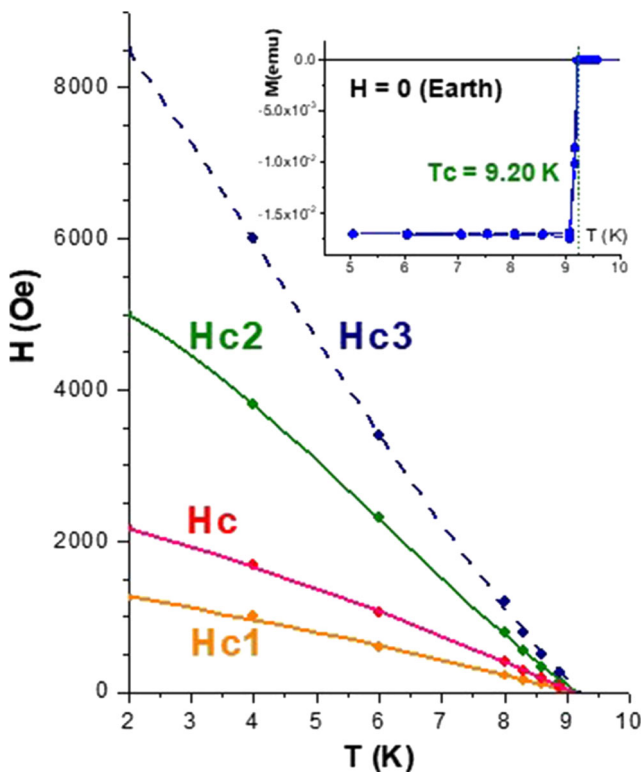


Fig. 5 Phase diagram of the single-crystal sample Nb-SC constructed from the $M(H)$ data measured in parallel field. H_{c1} , H_{c2} , and H_{c3} indicate the graphs for the respective critical fields and H_c is the graph for the thermodynamic critical field. Insert: magnetic moment measured at zero (Earth) field versus temperature

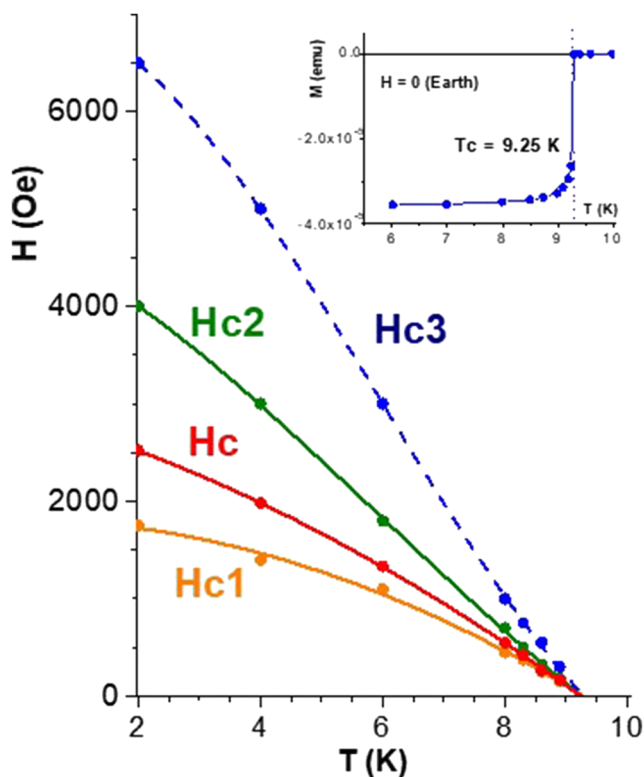


Fig. 6 Phase diagram of the film sample Nb-F. See captions of Fig. 5 for notations. Insert: magnetic moment measured at zero applied field versus temperature

Data for the magnetic moment measured in perpendicular field at high temperatures are shown in Figs. 7 and 8 for the Nb-SC and Nb-F samples, respectively. The data are reversible over more than half of the field range of the MS starting from H_{c2} . Therefore, in this range, the samples are in the equilibrium state. The equilibrium $M(H)$ are linear, and their extrapolation (represented by the dash-dotted green lines) to $H = 0$ yields $4\pi M(0)/V$ close to $-H_{c1}$ (shown by the red star) [43]. The validity of such an extrapolation is supported by the rule of 1/2: the area above the green line equals to the condensation energy $H_c^2 V/8\pi$ ($=1/2$ in coordinates $4\pi M/H_c V$ vs H/H_c), where H_c is calculated from the data obtained in parallel field.

Comparing Figs. 7 and 8 with Figs. 4 and 5 in [21], one notices a striking similarity in $M(H)$ for the MS and the IS. However, there are also important differences: in the IS, $M(0)/V$ and the critical field strongly depend on the sample thickness, whereas for both our samples, $4\pi M(0)/V$ is close to $-H_{c1}$ and $H_{c2\perp} = H_{c2\parallel}$, where $H_{c2\perp}$ and $H_{c2\parallel}$ are the upper critical fields in the perpendicular and the parallel geometries, respectively. Nevertheless, it was important to ensure that our samples are indeed type II superconductors. The most direct way for that is to measure the flux in the N domains.

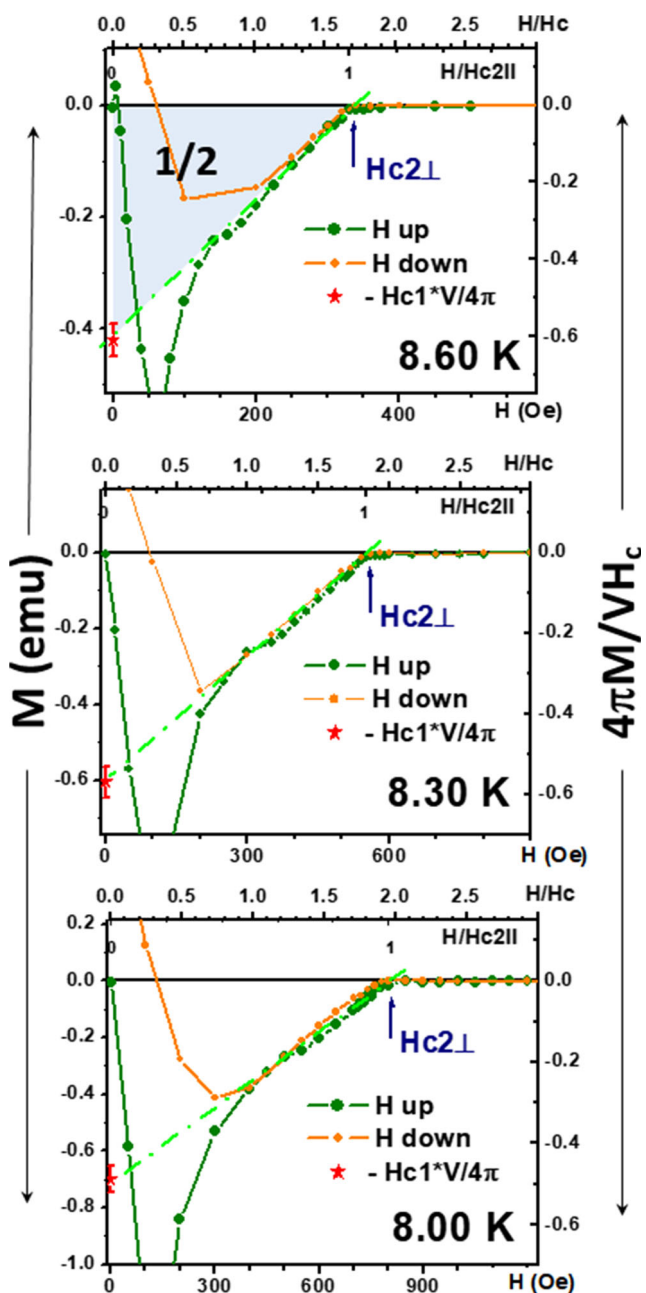


Fig. 7 Magnetic moment of the Nb-SC sample measured in perpendicular field at the indicated temperatures. The star shows $M(0) = -H_{c1}V/4\pi$ or $4\pi M(0)/V = -H_{c1}$ calculated using H_{c1} and V inferred from measurements in parallel field. Left and right vertical scales show M in different units as indicated; horizontal scales give the applied field in Oe (bottom), in units of $H_{c2||}$ (lower top) and in units of H_c (upper top). 1/2 designates the area above the green line representing the condensation energy $H_c^2V/8\pi$ (in coordinates $4\pi M/H_cV$ vs H/H_c) inferred from the data measured in parallel field

In the MS $\vec{B} = n\Phi_0$ [9], where the planar density $n = N/A$ is the number of flux lines N passing through an area A . In the transverse geometry, $\vec{B} = H$ and therefore

$$n = H/\Phi_0. \tag{3}$$

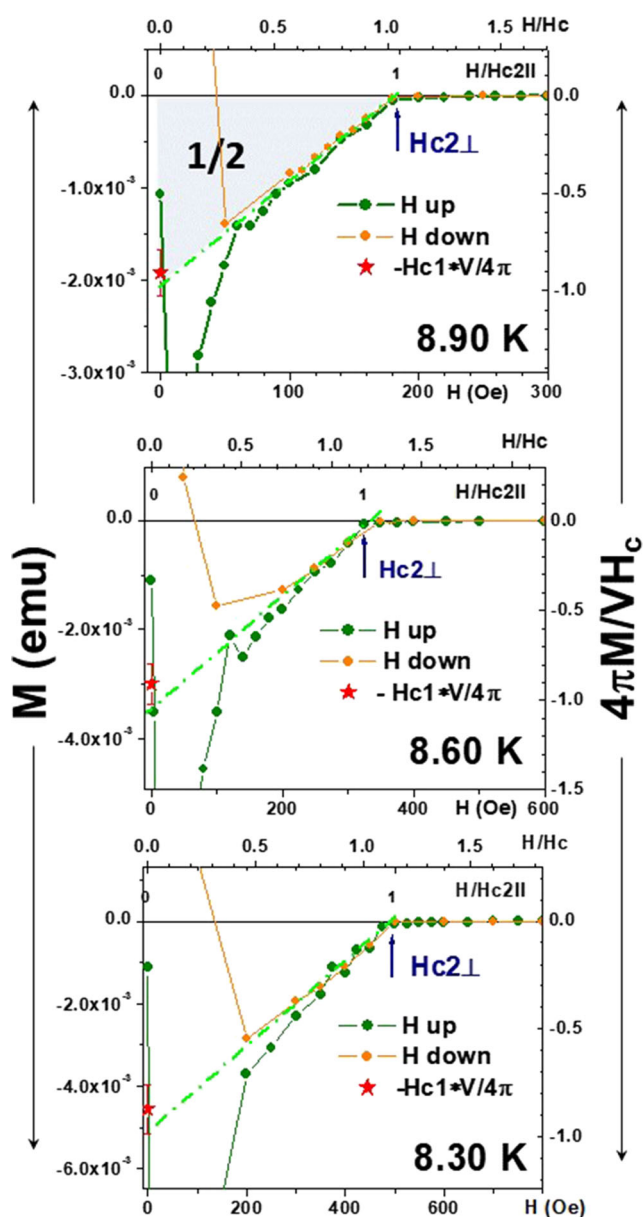
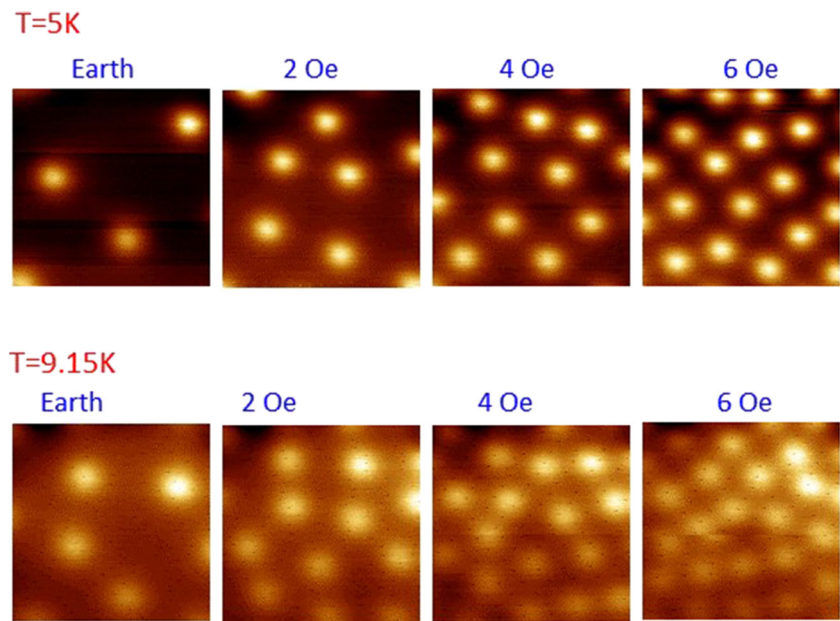


Fig. 8 Magnetic moment of Nb-F sample measured in perpendicular field at the indicated temperatures. See caption of Fig. 7 for details

Hence, the slope of $n(H)$ curve allows one to determine the flux in the N domains and therefore the type of superconductor.

With this in mind, we probed the film sample with a scanning Hall-probe microscope (SHPM) [44]. The scanned area was $7.6 \mu\text{m} \times 7.6 \mu\text{m}$ away from the sample edges. The sample was cooled at zero applied field. To achieve better resolution determined by the contrast of the field inside and outside the flux lines, the SHPM images were taken at low H . At low fields, pinning is *not small* (see Fig. 8, and Fig. 2a in [39]) and therefore the equilibrium hexagonal structure of the vortex ensemble can be mangled. Typical images taken at $T = 5.00$ and 9.15 K are shown in Fig. 9.

Fig. 9 Scanning Hall-probe images of the MS in Nb film taken at 5.00 K (upper row) and 9.15 K (lower row). The colors reflect relative magnitude of the induction with the brightest color corresponding to the strongest B . The bright spots are vortices. The fields in Oe indicated at the top of images are the applied field; the left images are taken at zero applied (Earth) field



A graph for $n - n_0 = (N - N_0)/A$ vs H is shown in Fig. 10. Here, N_0 is an adjustable parameter reflecting the occasional number of the lines in the scanned area at Earth field due to pinning and low statistics. As one can see, the experimental points agree with (3), thus confirming that each flux line carries a single flux quantum Φ_0 . Since κ of our single-crystal sample is larger than that of the film, we conclude that both our samples are classical type II superconductors with Abrikosov vortices [15].

4 Theoretical

The problem of the magnetic properties of inhomogeneous superconductors was for the first time addressed by Peierls [11] and F. London [12, 13] for the IS. As was mentioned above, both authors solved it in an averaged limit, in which

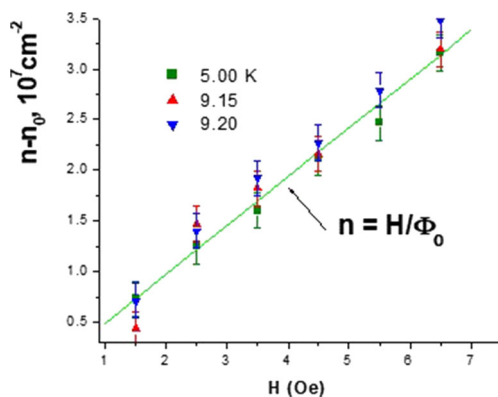


Fig. 10 Dependence of the flux line density n on the external field at different temperatures as indicated. Φ_0 is the superconducting flux quantum and n_0 is an adjustable parameter explained in the text

the non-uniform induction B is replaced by averaged \bar{B} , and using the demagnetizing factor η of the uniform sample. To supplement (1), Peierls and London assumed that $H_i = H_c$. This assumption was justified by a paradigm on instability of the N phase when $H_i < H_c$. Note, however, that this paradigm is valid only for the cylindrical geometry [35].

It is important to stress that the averaged description implies that the real sample structure is neglected and therefore any possible interactions between the structural units are neglected automatically. If, e.g., the sample consists of \aleph unit cells, then the sample free energy $F = \aleph \bar{F}_0$, where \bar{F}_0 is the average free energy per unit cell. Therefore, the averaged description does not contain cross terms responsible for interactions, hence excluding them by definition.

The Peierls-London model is valid for thick samples [2, 21, 35], i.e., when the surface-related inhomogeneities can be neglected (condition identical to that for the cylindrical geometry). Since N laminae are screened in the sample interior and interact through the outer field, neglect of the near-surface inhomogeneities means neglect of interaction between the laminae, in full consistency with the averaged approximation. Thus, the Peierls-London model represents a global description of the IS in a zero-order approximation [8], where interaction between the structural units is neglected.

For the MS, such an averaged model is missing, resulting in the absence of a global description of this state and leaving a significant “gap” in understanding the MS magnetic properties. In particular, as shown above, none of the existing theories is capable of addressing the magnetization curve for a slab in perpendicular field. The model, presented below, is targeted to fill this gap.

In Fig. 11, graphs for $\eta = 0$ represent the Maxwell field H_i vs H for the cylindrical geometry, where $H_i = H$.

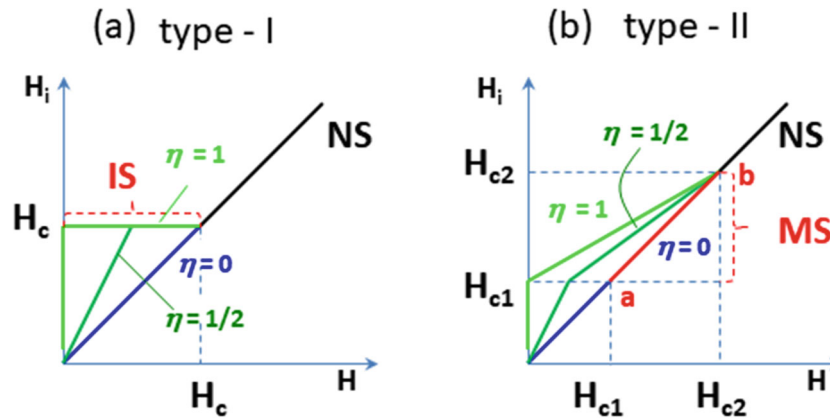


Fig. 11 Maxwell field H_i in type I (a) and type II (b) superconductors of different shapes vs external field H . Abbreviations NS, IS, and MS designate the normal, intermediate, and mixed states, respectively. Section ab in (b) represents $H_i(H)$ in the MS for samples with $\eta = 0$.

The demagnetizing factors η are related to a long cylinder and infinite slab in parallel field ($\eta = 0$), to a long circular cylinder in perpendicular field ($\eta = 1/2$), and to an infinite slab in perpendicular field ($\eta = 1$)

The red (ab) section in Fig. 11b represents this dependence for the MS, meaning that the function $H_i(H)$ is linear and extends from H_{c1} to H_{c2} . On the other hand, the experimental results for the transverse geometry (see Figs. 7 and 8), specifically (a) linear $M(H)$, (b) $H_{c2\perp} = H_{c2\parallel}$, and (c) $4\pi M(0)/V = -H_{c1}$, along with the condition $\bar{B} = H$, directly indicate [45] that $H_i(H)$ for $\eta = 1$ is also a linear function extending in the same range. Therefore, one can assume a linear form of $H_i(H)$ for all η , as it is shown in Fig. 11b. An analytical expression for these functions is

$$H_i = H_{c1} + \frac{H_{c2} - H_{c1}}{H_{c2} - H_{c1}(1 - \eta)}[H - H_{c1}(1 - \eta)]. \quad (4)$$

Having H_i , one obtains M from (2):

$$\frac{4\pi M}{V} = -H_{c1} + \frac{H_{c1}}{H_{c2} - H_{c1}(1 - \eta)}[H - H_{c1}(1 - \eta)], \quad (5)$$

then, $\bar{B} = H_i + 4\pi M/V$ is

$$\bar{B} = \frac{H_{c2}}{H_{c2} - H_{c1}(1 - \eta)}[H - H_{c1}(1 - \eta)]. \quad (6)$$

Graphs of these functions are presented in Fig. 12.

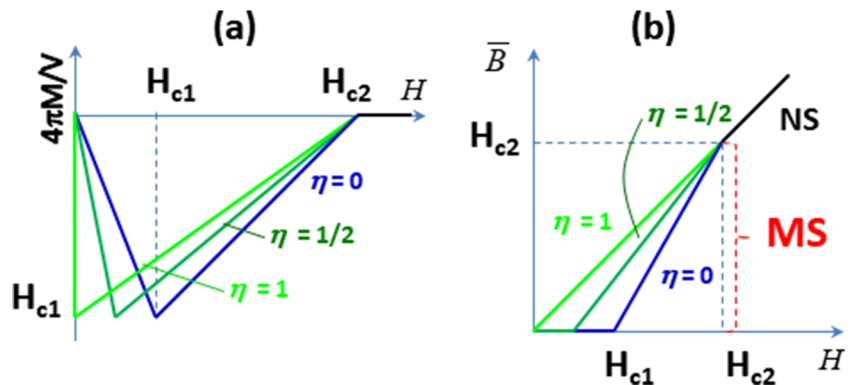
In type I materials, where by definition $H_{c1} = H_{c2} = H_c$ [22], (4) yields $H_i = H_c$, as in the Peierls-London model. This is easily seen from Fig. 11b: when $H_{c2} \rightarrow H_{c1}$, i.e., when a superconductor converts from type II to type I, the graphs in (b) convert to the graphs in (a). Then, (5) and (6) convert to formulas for M and \bar{B} in the Peierls-London model as well (see [21] for the graphs). Therefore, our model describes the averaged properties of both the MS and the IS in the limit of non-interacting vortices in type II superconductors and laminae in type I superconductors, respectively.

5 Discussion

First, we briefly stop at the rule of 1/2 because, being well known (see, e.g., [2]), it is not always clearly articulated in the textbooks. This rule represents the law of energy conservation in superconductors when \mathbf{M} is aligned (antiparallel) to \mathbf{H} . Consistency with this rule is a prerequisite for discussion of equilibrium properties.

In the general case, this law reads that, at constant T , the total free energy \tilde{F}_M (for which $\mathbf{M} = -\nabla_{\mathbf{H}}\tilde{F}_M$ [6]) of

Fig. 12 a Magnetic moment in terms of $4\pi M/V$ and b averaged induction \bar{B} versus external field H in type II superconductors with different demagnetizing factors η (see caption of Fig. 11 for explanation)



any singly connected superconductor of volume V in a dc magnetic field \mathbf{H} of any orientation is

$$\begin{aligned} \tilde{F}_M(H) &= \tilde{F}_M(0) - \int \mathbf{M}d\mathbf{H} \\ &= F_{S0} - \int \mathbf{M}d\mathbf{H} = F_{N0} - \frac{H_c^2 V}{8\pi} - \int \mathbf{M}d\mathbf{H}, \end{aligned} \quad (7)$$

where F_{S0} and F_{N0} are the Helmholtz free energies of the S and N states in zero field, respectively.

The first two forms of (7) show that the extra total free energy of a sample (above the free energy of the ground state $\tilde{F}_M(0) = F_{S0}$) is the sample magnetic energy $E_M = -\int \mathbf{M}d\mathbf{H}$, or the energy of interaction of the external field with the sample magnetic moment induced by this field. Similar as in conventional diamagnetics [14], E_M in superconductors is the kinetic energy of the charges (paired electrons) carrying the induced currents [2]. The last form of (7) demonstrates that (i) the total free energy in the N state ($= F_{N0}$) is independent of the external field since the magnetic permeability μ of this state is unity, and (ii) the source of E_M is the condensation energy $H_c^2 V/8\pi$. Finiteness of the latter makes a transition to the N state a mandatory property of any superconductor [6]. At this transition, E_M of any sample equals to its condensation energy or area under $M(H)$ curve plotted as $4\pi M/VH_c$ vs H/H_c , when \mathbf{M} is aligned to \mathbf{H} , is $1/2$. Therefore, the condensation energy density $H_c^2/8\pi$ is the energy per unit volume it takes to destroy superconductivity, i.e., to destroy an electron pairing [47].

As one can see from Fig. 12a, the area under the graphs $M(H)$ for different η is the same, meaning that if the magnetic moment is calculated for different orientations of the applied field, the sample condensation energy is the same, as it should. Therefore, our model meets the rule of $1/2$ and we can proceed to the discussion.

Comparing the modeled magnetization curve for $\eta = 1$ in Fig. 12a with the experimental data in Figs. 7 and 8, one can see that for the transverse geometry, the model is quantitatively consistent with the experiment.

Next, since the area under the graphs in Fig. 12a equals to $H_c^2/2$, we see that H_c is the geometrical mean of H_{c1} and H_{c2} , which is consistent with the rule known for the extreme type II limit [23]. This suggests that the rule $H_{c1}H_{c2} \approx H_c^2$ is more general than it looked till now.

Further, as shown by Andreev [46], in the IS, H_i is the Maxwell field and hence the induction in the N domains, where $B = \mu H_i = H_i$, since $\mu = 1$ in the N phase. Extending this consideration to the MS [22], one can state that H_i is the Maxwell field in the vortex cores. Therefore, our model suggests that B in the vortex cores increases from H_{c1} at $H = (1 - \eta)H_{c1}$ to H_{c2} at $H = H_{c2}$ and the structure of individual vortices (in sufficiently thick samples) does not depend on the sample shape (η).

Also, as seen from Fig. 11b, in the cores $B = H_i > H$ for all $\eta \neq 0$. This is consistent with the well-known fact (see, e.g., [48, 49]) that the upper boundary of μ SR measured spectrum of the magnetic induction in type II samples is greater than the external (perpendicularly directed) field.

However, there is an obvious problem. In Fig. 12a, the linear graph $M(H)$ for cylinders ($\eta = 0$) differs from the experimental curve, showing a non-linear change near H_{c1} (see, e.g., Fig. 3 or [17]). In the standard theory [8, 22, 23], this feature for cylindrical geometry (yielding the unrealistic infinite slope at H_{c1}) is described assuming overlapping the fields of neighboring vortices, leading to their repulsion. On the other hand, in cylinders, there is the surface current, which is *absent* in samples of the transverse geometry. The magnitude of this current is determined by the field drop at the surface [6], which is maximal near H_{c1} and vanishes upon approaching H_{c2} . Our model includes neither the vortex-vortex interaction, nor surface current, which explains the difference of the modeled and experimental $M(H)$ curves for $\eta = 0$. Note that surface current also is *not* accounted for in the standard theory [8, 22, 23].

The question then arises whether such a model is needed if vortices interact? The same question can be formulated as: Why for samples of the transverse geometry the experimental $M(H)$ graphs in Figs. 7 and 8 are identical to that in the model of non-interacting vortices in Fig. 12a? The only possible answer we can suggest for both formulations is because vortices in samples of the transverse geometry do not interact.

The field passes through any superconducting sample of the transverse geometry in which currents are optimized so to minimize the sample magnetic energy and therefore the total free energy \tilde{F}_M . However, the result of this optimization is different in type I and type II superconductors. Type I samples tune the period of the lamina structure, the fraction of the normal phase, and induction inside it, as well as the currents and the laminae shape near the surfaces, altogether leading to a strong dependence of the magnetic properties on the sample thickness d [21, 35].

No doubt that all these degrees of freedom are also available for type II superconductors, but owing to the gain received from the negative interface energy, in this case, all tunings are performed keeping maximum possible number of vortices and therefore the minimum flux passing through them, i.e., Φ_0 . Then, the vortex density n is as that in (3) and the parameter of the most effectively packed hexagonal vortex lattice $b = (2\Phi_0/\sqrt{3}H)^{1/2}$ [22].

It is important to stress that n and b are as such due to the symmetry and the flux conservation and, hence, do not depend on d .

On the other hand, if vortices in the transverse geometry do not interact, the sample magnetic energy is a simple sum of the free energies of the individual flux lines ϵd , where ϵ is the energy of the flux line per unit length (line tension).

Therefore, considering that $H = \bar{B} = n\Phi_0 = N\Phi_0/A$ and using (5) with $\eta = 1$ one obtains

$$\begin{aligned} E_M &= - \int \mathbf{M}d\mathbf{H} = N\epsilon d = \frac{V}{4\pi} H(H_{c1} - \frac{H_{c1}}{2H_{c2}}H) \\ &= Nd \frac{\Phi_0}{4\pi} (H_{c1} - \frac{H_{c1}}{2H_{c2}}H), \end{aligned} \quad (8)$$

which yields

$$\epsilon = \frac{\Phi_0 H_{c1}}{4\pi} (1 - \frac{H}{2H_{c2}}). \quad (9)$$

Comparing ϵ at H_{c1} in the cylinders ($= \Phi_0 H_{c1}/4\pi$ [8, 9, 22, 23]) with (9), we see that ϵ in the transverse geometry at $H \rightarrow 0$ when $H_i = H_{c1}$ equals to ϵ in the cylinders, as it should.

At higher field, ϵ decreases becoming $\Phi_0 H_{c1}/8\pi$ at $H=H_{c2}$, where it yields

$$E_M = N\epsilon d = (\frac{H_{c2}A}{\Phi_0})(\frac{\Phi_0 H_{c1}}{8\pi})d = \frac{H_{c1}H_{c2}}{8\pi} V = \frac{H_c^2}{8\pi} V, \quad (10)$$

as it should as well. Note that the latter is consistent with the physical meaning of the condensation energy density $H_c^2/8\pi$ as the energy needed to destroy pairing [47].

This confirms the validity of (9) and, hence, the absence of the interaction between vortices in samples with $\eta = 1$.

Therefore, the vortex matter in samples of the transverse geometry can be viewed as a peculiar 2D “gas-like” system of non-interacting vortices where the role of pressure P is taken by the external field H and the equation of state is given by (3) for the entire field range of the MS.

Indeed, similar to the gas, whose density $\rho \rightarrow 0$ when pressure $P \rightarrow 0$, and isothermal compressibility $\rho^{-1}(\partial\rho/\partial P)_T = 1/P$, the vortex matter is highly compressible, i.e., its density $n \rightarrow 0$ at $H \rightarrow 0$ and the “compressibility” $n^{-1}(\partial n/\partial H)_T = 1/H$. Similar to the gas, where the slope of ρ vs P is determined by the Boltzmann constant, in the vortex matter, the slope of n vs H is determined by the fundamental constant Φ_0 . But, contrary to the gas, the properties of the vortex matter do not depend on temperature. At constant sample temperature when the field H (“pressure”) changes, the vortex density n changes accordingly. But, when the field has stopped changing, vortices stay motionless, in contrast to the gas, where molecules continue thermal motion. Therefore, vortices in a slab in perpendicular field can be treated as a system at zero temperature. But, zero temperature means zero entropy. Therefore, vortices should be ordered in full consistency with well-known experimental fact [50].

Comparing the gas-like scenario with solid-like pictures [51], one can see that the former is more appropriate for the vortex matter since a primary property of solids, rigidity, is absent in the equilibrium vortex ensemble.

Now, we turn to one more aspect of our experimental results, i.e., the proximity of κ of our film sample to the critical value $\kappa_c = 1/\sqrt{2}$. In recent years, there emerged

an active interest in the properties of superconductors with $\kappa \approx \kappa_c$ (see [52] and references therein). Considering the properties of the critical ($\kappa = \kappa_c$) superconductors in the framework of classical field theory, Bogomol’nyi showed [53] that vortices with flux exceeding a single flux quantum are unstable against decay to single flux quantum vortices, and that the energy of a system of stable (single-flux-quantum) vortices equals to the sum of the energies of the unit vortex, i.e., vortices do not interact.

The GL parameter of our film sample is $1.1\kappa_c$, and, as we see, the vortices are indeed single-flux-quantum non-interacting units. The same was found for the Nb-SC sample with $\kappa = 1.8\kappa_c$. Hence, our experimental results confirm Bogomol’nyi’s predictions for superconductors with $\kappa \gtrsim 1/\sqrt{2}$.

Finally, we have to address a question inevitably arising when reading this paper: if vortices do not interact when the sample (e.g., a film) is in perpendicular field, why do they interact when the field is parallel, as stated in the standard theory? In view of enormous amount of literature associated with the vortex interaction, a complete answer to this question is hardly feasible in the framework of this paper. Therefore, what follows should be sooner considered as an invitation to discussion than a solid judgment on this matter.

The vortex-vortex interaction in the standard theory follows from the *assumption* of overlapping of the inductions B of neighboring vortices, which increases the sample free energy thus leading to repulsive interaction between vortices [8, 22, 23]. Note, however, that overlapping of B at some point inside the sample means overlapping of currents at the same point, i.e., overlapping of vortices [55]. The latter is met neither in normal fluids [56] nor in superfluids [57, 58]. In the GL theory, vortices in superconductors also do not overlap [15, 59].

Indeed, in regular matter, overlapping of electron shells of neighboring molecules results in strong molecular repulsion leading to practical incompressibility of liquids and solids. As we have seen, this is not the case for the vortex matter in superconductors. This is because molecules are fixed entities, whereas vortices are self-adjustable units. Recall that currents induced in a singly connected superconductor serve *solely* to reduce its free energy. Therefore, since the B overlapping increases the free energy, one can expect that the superconductor will tune the currents to avoid that, thus keeping vortices non-interacting regardless of the vortex density. This qualitative scenario is consistent with the reported experimental results for the transverse geometry and, most importantly, with the rule of 1/2, valid for all geometries and indicating that the total free energy of superconductors contains no potential energy.

Coming back to our model of zero-order approximation, we note that it does not include inhomogeneities near the “transverse” (perpendicular to the field) sample surface, as

it also takes place in the Peierls-London model for the IS. These inhomogeneities increase the sample magnetic energy and therefore modify the magnetization curve. In particular, as it was mentioned above, in the IS, they can significantly decrease the upper critical field [21]. However, contrary to the IS, where effects of these inhomogeneities were noticed already in 2-mm thick samples [54], such effects were not found in our samples. This can be explained by a finer pattern of these inhomogeneities (compare images in Fig. 9 with those in [35]). Therefore, the surface-related effects in the MS should be expected in thinner samples and they may differ from those in the IS, hence constituting a very interesting problem of fundamental superconductivity.

6 Summary and Outlook

Equilibrium properties of the mixed state in type II superconductors were studied with high-purity film and single-crystalline niobium samples with zero and unity demagnetizing factor η , that is in parallel and perpendicular magnetic fields, respectively. The magnetization curve for the samples with $\eta = 1$ was obtained for the first time. It was found that existing theories fail to describe these new data. A theoretical model successfully addressing this problem was developed and experimentally validated.

The new model describes magnetic properties of the mixed state in a zero-order approximation where interactions between vortices and surface current are ignored. The model is applicable to thick samples with any η without limitation for the magnitude of the Ginzburg-Landau parameter κ . The model is quantitatively consistent with the data obtained for the samples with $\eta = 1$, where the surface current is absent by definition. This indicates the absence of interaction between vortices in such samples. An expression for the field strength H_i inside superconductors in the mixed state is obtained together with a formula for the line tension of vortices valid in the entire field range of the mixed state. At low κ , our model converts to that of Peierls and London for the intermediate state in type I superconductors, which is valid in the limit of non-interacting laminae. It is shown that visualization of the vortex matter as an ordered 2D gas-like system at zero temperature is more appropriate than the frequently used solid-like scenarios.

The reported model is constructed and verified using experimental results obtained with low- κ Nb type II superconductors. Therefore, it is interesting and important to test the model with materials of higher κ . Single-crystal samples of A15 compounds, e.g., V_3Si , can be appropriate candidates for such a verification. Single-crystal samples of unconventional superconductors close to the critical temperature can be also appropriate.

Acknowledgments We express deep gratitude to Michael E. Fisher and Konstantin A. Kikoin for valuable remarks, and to Yurii M. Kagan for encouraging comments on the manuscript. We are thankful to Oscar Bernal, Connie Hebert, and Andrew MacFarlane for their crucial help in organizing the project.

Funding Information This work was supported in part by the National Science Foundation (Grant No. DMR 0904157), by the Research Foundation – Flanders (FWO, Belgium) and by the Flemish Concerted Research Action (BOF KU Leuven, GOA/14/007) research program. V.K. acknowledges support from the sabbatical fund of the Tulsa Community College. A.-M. Valente-Feliciano is supported by the U.S. Department of Energy, Office of Science, Office of Nuclear Physics under contract DE-AC05-06OR23177.

References

- Shubnikov, L.V., Khotkevich, V.I., Shepelev, Y.D., Ryabinin, Y.N.: Magnetic properties of superconducting metals and alloys. *Zh.E.T.F.* **7**, 221–237 (1937)
- Shoenberg, D. *Superconductivity*, 2nd Ed. Cambridge University Press, Cambridge (1952)
- Serin, B.: Type-II superconductors. Experiment. In: Parks, R.D. (ed.) *Superconductivity*, V. 2. Marcel Dekker Inc., N.Y (1969)
- Brandt, E.H.: The flux-line lattice in superconductors. *Rep. Prog. Phys.* **58**, 1465–1589 (1995)
- Zeldov, E.: Vortex matter in superconductors. In: Rogalla, H., Kes, P. (eds.) *100 Years of Superconductivity*, pp. 222–231. CRC Press, Boca Raton (2012)
- Landau, L.D., Lifshitz, E.M., Pitaevskii, L.P. *Electrodynamics of Continuous Media*, 2nd ed. Elsevier, Amsterdam (1984)
- Maxwell, J.C. *A Treatise on Electricity and Magnetism V*, 2nd ed, vol. II. Clarendon Press, Oxford (1881)
- de Gennes, P.G.: *Superconductivity of Metals and Alloys*. Westview, Boulder, CO (1966)
- Abrikosov, A.A.: *Fundamentals of the Theory of Metals*. Elsevier Science Pub. Co., Amsterdam (1988)
- Kozhevnikov, V., Valente-Feliciano, A.-M., Curran, P., Richter, G., Liu, H., Volodin, A., Bending, S., Van Haesendonck, C.: Abstract E25.00009, *Bulletin of the American Physical Society*. 61(2). First results of this study were presented at APS March Meeting in 2016 (2016)
- Peierls, R.: Magnetic transition curves of supraconductors. *Proc. Roy. Soc. London, Ser. A.* **155**, 613–627 (1936)
- London, F.: Zur theorie magnetischer felder im supraleiter, **3**, 450–459 (1936)
- London, F. *Superfluids*, 2nd ed, vol. 1. Dover, N.Y. (1961)
- Tamm, I.E. *Fundamentals of the Theory of Electricity*, 9th ed. Nauka, Moscow (1976). English translation: Mir, Moscow, (1979)
- Abrikosov, A.A.: On the magnetic properties of superconductors of the second group. *Zh.E.T.F.* **32**, 1442–1452 (1957)
- Livingston, J.D.: Magnetic properties of superconducting lead-based alloys. *Phys. Rev.* **129**, 1943–1949 (1963)
- Finnemore, D.K., Stromberg, T.F., Swenson, C.A.: Superconducting properties of high-purity niobium. *Phys. Rev.* **149**, 231–243 (1966)
- French, R.A., Lowell, J., Mendelsohn, K.: Almost ideal behavior in some type-II superconducting alloys. *Cryogenics* **7**, 83–88 (1967)
- French, R.A.: Intrinsic type-2 superconductivity in pure niobium. **8**, 301–308 (1968)

20. In normal dia- and paramagnetics, magnetization m is defined as magnetic moment per unit volume caused by microscopic (molecular) persistent currents averaged over physically infinitesimal volume [14]. In superconductors this definition loses sense due to much greater spatial scale of the persistent currents and therefore m is used only as M/V [6]
21. Kozhevnikov, V., Van Haesendonck, C.: Magnetic moment of a slab of type-I superconductor: theoretical model and experiment. *Phys. Rev. B* **90**, 104519 (2014)
22. Lifshitz, E.M., Pitaevskii, L.P.: *Statistical Physics v.2*, Nauka M (1973)
23. Tinkham, M. *Introduction to Superconductivity*, 2nd ed. Dover Publication, Mineola (1996)
24. Koppe, H., Willebrand, J.: Approximate calculation of the reversible magnetization curve of type II superconductors. *J. Low-Temp. Phys.* **2**, 499–506 (1970)
25. Brandt, E.H.: Precision Ginzburg-Landau solution of ideal vortex lattices for any induction and symmetry. *Phys. Rev. Letters* **78**, 2208–2211 (1999)
26. Chang, G.K., Tinsel, T., Serin, B.: Magnetic transition of a superconducting film in a transverse field. *Phys. Lett.* **5**, 11–13 (1963)
27. Miller, P.B., Kington, B.W., Quinn, D.J.: Transverse magnetization of In-Sn films. *Rev. Mod. Phys.* **36**, 70–73 (1964)
28. Cody, G.D., Miller, R.E.: Magnetic transitions of superconducting thin films and foils. I. Lead. *Phys. Rev.* **173**, 481–494 (1968)
29. Fetter, A.L., Hohenberg, P.C. In: Parks, R.D. (ed.): *Theory of Type-II Superconductors in Superconductivity*, vol. 2. Marcel Dekker, Inc., N.Y. (1969)
30. In [8] this expression is erroneously given as $H_i = (H - B/4\pi)/(1 - \eta/4\pi)$.
31. Landau, L.D.: On the theory of superconductivity. *Zh.E.T.F.* **7**, 371–380 (1937)
32. Equality $\bar{B} = H$ for an infinite plate in a perpendicular field ($\eta = 1$) can be easily understood from the flux conservation. In this case all field lines issued by a magnet pass through a superconducting plate as it also takes place for a normal metallic plate. This means that for the magnet it does not matter either this sample is below the critical temperature T_c , that is superconducting, or above T_c , that is in the normal state, where $B = H$ by definition.
33. Brandt, E.H.: Ginzburg-landau vortex lattice in superconductor films of finite thickness. *Phys. Rev. B* **71**, 014521 (2005)
34. Doria, M.M., Brandt, E.H., Peeters, F.M.: Magnetization of a superconducting film in a perpendicular magnetic field. *Phys. Rev. B* **78**, 054407 (2008)
35. Kozhevnikov, V., Wijngaarden, R.J., de Wit, J., Van Haesendonck, C.: Magnetic flux density and the critical field in the intermediate state of type-I superconductors. **89**, 100503(R) (2014)
36. Cribier, D., Jacrot, B., Madhav Rao, L., Farnoux, B.: Mise en évidence par diffraction de neutrons d'une structure périodique du champ magnétique dans le niobium supraconducteur. *Phys. Lett.* **9**, 106–107 (1964)
37. Laver, M., Forgan, E.M., Brown, S.P., Charalambous, D., Fort, D., Howell, C., Ramos, S., Lycett, R.J., Christen, D.K., Kohlbrecher, J., Dewhurst, C.D., Cubitt, R.: Spontaneous symmetry-breaking vortex lattice transitions in pure niobium. *Phys. Rev. Lett.* **96**, 167002 (2006)
38. Maisuradze, A., Nakai, N., Machida, K., Khasanov, R., Amato, A., Biswas, P.K., Baines, C., Herlach, D., Henes, R., Keppler, P., Keller, H.: Magnetic field distribution and characteristic fields of the vortex lattice for a clean superconducting niobium sample in an external field applied along a three-fold axis. *Phys. Rev. B* **89**, 184503 (2014)
39. Kozhevnikov, V., Valente-Feliciano, A.-M., Curran, P.J., Suter, A., Liu, A.H., Richter, G., Morenzoni, E., Bending, S.J., Van Haesendonck, C.: Equilibrium properties of superconducting niobium at high magnetic fields: a possible existence of a filamentary state in type-II superconductors. *Phys. Rev. B* **95**, 174509 (2017)
40. Wu, G., Valente, A.-M., Phillips, H.L., Wang, H., Wu, A.T., Renk, T.J., Provencio, P.: Studies of niobium thin film produced by energetic vacuum deposition. *Thin Solid Films* **489**, 56–62 (2005)
41. Casalbuoni, S., Knabbe, E.C.A., Kotzler, J., Lilje, L., von Sawilski, L., Schmuser, P., Steffen, B.: Surface superconductivity in niobium for superconducting RF cavities. *Nuclear Instruments and Methods in Physics Research A: Accelerators, Spectrometers, Detectors and Associated Equipment* **538**, 45–64 (2005)
42. Valente-Feliciano, A.-M.: Development of SRF monolayer/multilayer thin film materials to increase the performance of SRF accelerating structures beyond bulk Nb. PhD dissertation Universit Paris Sud - Paris XI (2014)
43. $M(0)$ is the magnetic moment at $H \rightarrow 0$
44. Oral, A., Bending, S.J., Henini, M.: Real-time scanning Hall probe microscopy. *Phys. Lett.* **69**, 1324–1326 (1996)
45. $H_i(H) = \bar{B}(H) - 4M(H)/V = H - 4M(H)/V$, hence linear $M(H)$ means linear $H_i(H)$
46. Andreev, A.F.: Electrodynamics of the intermediate state. *Zh.E.T.F.* **51**, 1510–1521 (1966)
47. Kresin, V.Z., Wolf, S.A.: *Fundamentals of Superconductivity*. Plenum Press, N.Y. (1990)
48. Sonier, J.E., Brewer, J.H., Kief, R.F.: μ SR studies of the vortex state in type-II superconductors. *Rev. Mod. Phys.* **72**, 769–811 (2000)
49. Niedermayer, C.h., Forgan, E.M., Gluckler, H., Hofer, A., Morenzoni, E., Pleines, M., Prokscha, T., Riseman, T.M., Birke, M., Jackson, T.J., Litterst, J., Long, M.W., Luetkens, H., Schatz, A., Schatz, G.: Direct observation of a flux line lattice field distribution across an $YBa_2Cu_3O_7$ surface by Low Energy Muons. *Phys. Rev. Lett.* **83**, 3932–3935 (2002)
50. Essmann, U., Trauble, H.: The direct observation of individual flux lines in type-II superconductors. *Phys. Lett.* **24A**, 526–527 (1967)
51. Blatter, G., Feigel'man, M.Y., Geshkenbein, Y.B., Larkin, A.I., Vinokur, V.M.: Vortices in high-temperature superconductors. *Rev. Mod. Phys.* **66**, 1125–1388 (1994)
52. Lukyanchuk, I., Vinokur, V.M., Rydh, A., Xie, R., Milosevic, M.V., Welp, U., Zach, M., Xiaok, Z.L., Crabtree, G.W., Bending, S.J., Peeters, F.M., Kwok, W.K.: Rayleigh instability of confined vortex droplets in critical superconductors. *Nature Phys.* **11**, 21–25 (2015)
53. Bogomolnyi, E.B.: The stability of classical solutions. *J. Nucl. Phys.* **24**, 449–454 (1976)
54. Sharvin, Y.V.: Measurements of surface tension at the boundary between superconducting and normal phases. *Zh.E.T.F.* **33**, 1341–1346 (1957)
55. Inhomogeneous B throughout the sample in the MS [15], implies spatial variation of the tangential component of the vector B . In absence of a transport current, the latter may occur only due to a current making closed loops in the plane perpendicular to B [6, 14], i.e. the current in vortices.
56. Landau, L.D., Lifshitz, E.M. *Fluid Mechanics*, 2nd ed. Elsevier, Amsterdam (1987)
57. Feynman, R.P.: Application of Quantum Mechanics to Liquid Helium. In: Gorter, C.J. (ed.) *Progress in Low Temperature Physics*, vol. I, pp. 17–53. North Holland Publishing Company, Amsterdam (1955)
58. Yarmchuk, E.J., Packard, R.E.: Photographic studies of quantized vortex lines. *J. Low Temp. Phys.* **46**, 479–515 (1982)
59. Brandt, E.H.: Properties of the ideal Ginzburg-Landau vortex lattice. *Phys. Rev. B* **68**, 054506 (2003)